An atypical active cell death process underlies the fungicidal activity of ciclopirox olamine against the yeast *Saccharomyces cerevisiae*

Bruno Almeida[1], Belém Sampaio-Marques[1], Joana Carvalho[1], Manuel Silva[2], Cecília Leão[1], Fernando Rodrigues[1] & Paula Ludovico[1]

[1]Life and Health Sciences Research Institute (ICVS), Health Sciences School, University of Minho, Campus de Gualtar, Braga, Portugal; and [2]Instituto de Biologia Molecular e Celular (IBMC), Porto, Portugal

Correspondence: Paula Ludovico, Life and Health Sciences Research Institute, Health Sciences School, University of Minho, Campus de Gualtar, 4710-057 Braga, Portugal. Tel.: +351 253604812; fax: +351 253604809; e-mail: pludovico@ecsaude.uminho.pt

Received 28 March 2006; revised 5 July 2006; accepted 23 October 2006.

DOI:10.1111/j.1567-1364.2006.00188.x

Editor: Ian Dawes

Keywords
ciclopirox olamine; active cell death; reactive oxygen species; proteases; caspase-independent cell death.

Abstract

Ciclopirox olamine (CPO), a fungicidal agent widely used in clinical practice, induced in *Saccharomyces cerevisiae* an active cell death (ACD) process characterized by changes in nuclear morphology and chromatin condensation associated with the appearance of a population in the sub-G_0/G_1 cell cycle phase and an arrest in the G_2/M phases. This ACD was associated neither with intracellular reactive oxygen species (ROS) signaling, as revealed by the use of different classes of ROS scavengers, nor with a terminal deoxynucleotidyl transferase-mediated dUTP nick end labeling (TUNEL)-positive phenotype. Furthermore, CPO-induced cell death seems to be dependent on unknown protease activity but independent of the apoptotic regulators Aif1p and Yca1p and of autophagic pathways involving Apg5p, Apg8p and Uth1p. Our results show that CPO triggers in *S. cerevisiae* an atypical nonapoptotic, nonautophagic ACD with as yet unknown regulators.

Introduction

Ciclopirox olamine (CPO) belongs to a group of synthetic antifungal agents, hydroxypyridones, that are used effectively in clinical practice and that have a very broad spectrum of action against dermatophytes, yeast, filamentous fungi and bacteria (Sakurai *et al.*, 1978b; Abrams *et al.*, 1991; Kokjohn *et al.*, 2003). In addition, this drug has been frequently used with remarkable success against azole-resistant *Candida* species (Niewerth *et al.*, 2003). Although hydroxypyridones have been used in clinical practice for the last 30 years, their mode of action is still poorly understood. Nonetheless, it is well established that, in contrast to other antifungal agents such as azoles or polyenes, hydroxypyridones do not produce antifungal activity by inhibition of ergosterol synthesis (Gupta, 2001). CPO is well known as a chelating agent that forms complexes with iron cations such as Fe^{3+}, inhibiting the iron-containing enzymes, such as catalase and peroxidase, that play a part in the intracellular degradation of toxic peroxides (Niewerth *et al.*, 2003). Nevertheless, CPO protects mitochondria from hydrogen peroxide toxicity mainly by inhibiting mitochondrial membrane potential depolarization (Lee *et al.*, 2005b). CPO treatment induces the expression of many genes involved in iron uptake in *Candida albicans* cells (Lee *et al.*, 2005a), which is consistent with CPO acting as an iron chelator. CPO also inhibits uptake of precursors of macromolecule biosynthesis by *C. albicans* (Sakurai *et al.*, 1978b; Iwata & Yamaguchi, 1981), but did not affect endogenous respiration, and therefore interference with electron transport was not suspected to be the primary cause of its antifungal activity (Sakurai *et al.*, 1978a). Intracellular CPO is neither metabolized nor degraded (Sakurai *et al.*, 1978b), with 97% of the accumulated drug binding irreversibly to the cell membrane, cell wall, mitochondria and ribosomes, and small amounts being found free in the cytosol. Transmission electron microscopy (TEM) studies conducted on CPO-treated *C. albicans* cells showed enlargement of the vacuole and mitochondria, and invagination of the plasma membrane, whereas the cell wall remained unaffected (Niewerth *et al.*, 2003). It was recently shown that the targets of CPO in *Saccharomyces cerevisiae* include many proteins that participate in different aspects of cellular metabolism, such as DNA replication, DNA repair, signal transduction, and cellular transport (Leem *et al.*, 2003).

A significant feature of CPO is that no single case of fungal resistance has been reported so far, even though it was

FEMSYR 188.PDF 29-Nov-06 18:43 506267 Bytes 9 PAGES n operator=Christina)

	FEMSYR	188	B	Dispatch: 29.11.06 Journal: FEMSYR	CE: Bhavani
	Journal Name	Manuscript No.		Author Received: No. of pages: 9	PE: Chris/Saravanan

©WUK FEMSYR 188

introduced into clinical therapy more than three decades ago. Niewerth *et al.* (2003) demonstrated that even the upregulation of well-characterized multidrug resistance genes, e.g. *CDR1*, *CDR2* and *FLU1*, or 6 months of exposure to the drug could not generate CPO resistance in *C. albicans*. Our knowledge of the fungal targets of this clinically established and very efficient drug, which has very few side effects when used topically, is poor (Gupta, 2001). Because of its genetic tractability and easy laboratory handling, we used *S. cerevisiae* as a model to evaluate the mechanisms of the antifungal action of CPO. In particular, we aimed to determine whether CPO triggers an active cell death (ACD) pathway, as recently shown for *C. albicans* cells treated with amphotericin B (Phillips *et al.*, 2003). For this purpose, we evaluated CPO effects on several cellular parameters, such as mitochondrial function/integrity, plasma membrane integrity, cell cycle progression, reactive oxygen species (ROS) production, nuclear morphology, DNA fragmentation, autophagy and caspase-like or aspartic protease (ASPase) activity.

Materials and methods

Microorganisms and growth conditions

The yeast *S. cerevisiae* strain BY4742 (*MAT*Δ*his3*Δ1 *leu2*Δ0 *lys2*Δ0 *ura3*Δ0), susceptible to CPO concentrations higher than 16 μg mL^{-1}, and the respective knockouts in *YCA1*, *AIF1*, *APG5*, *APG8* and *UTH1* genes were used in the experiments. The growth experiments were performed in liquid YEPD medium in 300-mL flasks containing a 2 : 1 air-to-liquid phase ratio, and incubated on a mechanical shaker (150 r.p.m.) at 26 °C. Cells were grown to early stationary growth phase (2.5 $OD_{640\,nm}$). For specific experiments, cells were grown to exponential (0.8 $OD_{640\,nm}$) or stationary (3.5 $OD_{640\,nm}$) growth phase. OD was measured in a 'Sprectronic GENESYS 20' (Thermo Electron Corporation) spectrophotometer.

Treatments with CPO and inhibition of protein synthesis

Early stationary-phase cells were harvested and suspended (10^6 cells mL^{-1}) in YEPD medium containing 0, 16, 18, 20 and 22 μg mL^{-1} CPO (SIGMA C-0415). The treatments were carried out for 200 min at 26 °C with shaking (150 r.p.m.). The cellular effects of CPO on plasma membrane integrity, mitochondrial function/integrity and ROS production were kinetically analyzed (0, 60, 90, 120, 200 and 240 min) by flow cytometry as described hereafter. The inhibition of protein synthesis was performed by adding cycloheximide (Merck), 100 μg mL^{-1} (Ludovico *et al.*, 2001b), to the cell suspensions at the same time as CPO. Cycloheximide at this concentration did not affect *S. cerevisiae* viability after 200 min of incubation. Cell viability was determined by CFU counts after 2 days of incubation at 26 °C on YEPD agar plates. No further colonies appeared after that incubation period. The relative survival percentages were calculated, with 100% of viability corresponding to 1.11×10^6 cells.

Flow cytometry assays

Flow cytometry assays were performed on an EPICS XL-MCL (Beckman-Coulter Corporation, Hialeah, FL) flow cytometer, equipped with an argon-ion laser emitting a 488-nm beam at 15 mW. The green and red fluorescences were collected through a 488-nm blocking filter, a 550-nm long-pass dichroic^{-1} with a 525-nm bandpass^{-1} and a 590-nm long-pass^{-1} with a 620-nm bandpass^{-1}, respectively. Twenty thousand cells per sample were analyzed. The data were evaluated with the MULTIGRAPH software included in the system II acquisition software for the EPICS XL/XL-MCL version 1.0.

Cell-sorting assays were performed on a BD FACSAria Cell Sorting System (BD Biosciences, San Jose, CA), using a Coherent Sapphire solid-state laser at 488 nm. Separation of cells was carried out at a medium sheath pressure of 26 p.s.i. and a frequency of 60 kHz. Data were analyzed using FACSDIVA software.

Assessment of plasma membrane integrity

Plasma membrane integrity was assessed by flow cytometry using propidium iodide (PI) (Molecular Probes, Eugene, OR) vital staining as described elsewhere (de la Fuente *et al.*, 1992) with minor adaptations. Briefly, PI was added to yeast cell suspensions (10^6 cells mL^{-1}) from a working solution (0.5 mg of PI in 10 mL of Tris/$MgCl_2$ buffer) to a final concentration of 6.7 μg mL^{-1} and incubated at 37 °C for 15 min. Cells with high red fluorescence were considered to have plasma membrane disruption.

Assessment of mitochondrial function/integrity and ROS production

Mitochondrial function/integrity was evaluated by flow cytometry using the fluorescent dye rhodamine 123 (Rh123) (Molecular Probes, Eugene, OR), as described elsewhere (Ludovico *et al.*, 2001a). Briefly, cells presenting green fluorescence levels identical to those presented by heat-killed cells were considered to have disturbances in mitochondrial function/integrity.

Cellular ROS production was kinetically monitored by flow cytometry with MitoTracker Red CM-H_2XRos (Molecular Probes) staining, as previously described (Ludovico *et al.*, 2002). Cells presenting high red fluorescence were considered to have increased intracellular ROS concentrations.

CPO treatment was carried out in the presence of different classes of ROS scavengers. Ascorbic acid (10 mM), glutathione (5 mM) and acetyl-L-carnitine (0.02 g L^{-1}) were added to the cell suspension before addition of CPO. At

these concentrations, antioxidants did not affect *S. cerevisiae* viability after 200 min of incubation (data not shown).

Cell cycle analysis

Cell cycle analysis was performed after treatment with 18 and 20 μg mL^{-1} CPO, as described elsewhere (Fortuna *et al.*, 2000). Briefly, at the desired time points, cells were harvested, washed and fixed with ethanol (70% v/v) for 30 min at 4 °C, and this was followed by sonication, treatment with RNAse for 1 h at 50 °C in sodium citrate buffer (50 mM sodium citrate, pH 7.5), and subsequent incubation with proteinase K (0.02 mg 10^{-7} cells). Cell DNA was then stained overnight with SYBR Green 10 000 × (Molecular Probes), diluted 10-fold in Tris-EDTA (pH 8.0), and incubated overnight at 4 °C. Before cytometric analysis, samples were diluted 1 : 4 in sodium citrate buffer. Determination of cells in each phase of the cell cycle was performed offline with MODFIT LT software (Verity Software House, Topsham, ME).

Assessment of nuclear morphology alterations and terminal deoxynucleotidyl transferase-mediated dUTP nick end labeling (TUNEL) assay

Changes in the nuclear morphology of CPO-treated *S. cerevisiae* cells were assessed by 4,6-diamino-2-phenyl-indole dihydrochloride (DAPI) staining. CPO-treated cells were harvested, washed, and resuspended in phosphate-buffered saline (PBS) with DAPI (0.5 μg mL^{-1}) for 10 min. Stained cells were washed twice with PBS and visualized by epifluorescence microscopy with an Olympus BX61 microscope with filter wheels, to control excitation and emission wavelengths, equipped with a high-resolution Olympus DP70 digital camera. DNA strand breaks were assessed by a TUNEL assay with the *In situ* Cell Death Detection Kit, Fluorescein (Roche Applied Science, Indianapolis, IN) as described elsewhere (Ludovico *et al.*, 2001b).

Caspase-like or ASPase activity

Caspase-like or ASPase activity was detected using a CaspSCREEN Flow Cytometric Analysis Kit (Chemicon). Cells were incubated with the nonfluorescent substrate D_2R at 37 °C for 45 min, and then analyzed by flow cytometry and epifluorescence microscopy. Micrographs were acquired in an Olympus BX61 microscope with filter wheels, to control excitation and emission wavelengths, equipped with a high-resolution Olympus DP70 digital camera.

TEM analysis and confocal microscopy

Cells from different treatment conditions were washed with phosphate/magnesium buffer (40 mM K_2HPO_4/KH_2PO_4, pH 6.5, 0.5 mM $MgCl_2$), suspended in 2.5% (v/v) glutaraldehyde in 40 mM phosphate/magnesium buffer (pH 6.5), and fixed overnight at 4 °C. After fixation, the cells were rinsed twice in 0.1 M phosphate/citrate buffer (pH 5.8) and suspended in this buffer containing 10 U mL^{-1} lyticase (Boehringer Mannheim) for about 90 min at 37 °C, to digest the cell wall. After cell wall digestion of the prefixed yeast cells, protoplasts were washed and postfixed with 2% (w/v) osmium tetroxide (2 h), and this was followed by 30 min of incubation with 1% (w/v) aqueous uranyl acetate (Silva *et al.*, 1987). Dehydration was performed as described by Byers & Goetsch (1991) for embedding vegetatively grown yeast cells. After 100% ethanol washes, the samples were transferred to 100% propylene oxide, and incubated with 50% (v/v) propylene oxide and 50% (v/v) Epon (TAAB Laboratories) for 30 min and with 100% Epon overnight. Cells were transferred to gelatin capsules with 100% Epon and incubated at 60 °C for 48 h before cutting thin sections and staining with uranyl acetate and lead acetate. Micrographs were taken with a Zeiss EM 10C electron microscope.

The images in Fig. 2c were acquired in a confocal Olympus FLUOVIEW microscope with an Olympus PLAPON 60X/oil objective, with a numerical aperture of 1.42, and using the Olympus FLUOVIEW advanced software.

Reproducibility of the results

The results presented are mean values and SDs of at least three independent assays. Statistical analyses were carried out using independent samples *t*-tests. A *P*-value less than 0.05 was assumed to denote a significant difference.

Results and discussion

CPO induces *S. cerevisiae* ACD

Exposure of *S. cerevisiae* to CPO resulted in dose-dependent cell death (Fig. 1a). As reported in other instances of *S. cerevisiae* ACD (Madeo *et al.*, 1999; Ludovico *et al.*, 2001b), CPO-induced cell death was attenuated by coincubation with the protein synthesis inhibitor cycloheximide (Fig. 1a). In addition, these results were shown to be independent of cell growth phase: exponential, early stationary, and stationary (Fig. 1b). Moreover, the addition of cycloheximide after 20 min of CPO treatment still abrogated cell death, showing that death occurs via a mechanism other than the inhibition of CPO uptake (data not shown).

The plasma membrane is one of the main targets of many antifungal agents (Groll *et al.*, 1998; Theis & Stahl, 2004). PI staining showed alterations in plasma membrane integrity in 23% and 41% of cells when they were treated with 18 and 20 μg mL^{-1} CPO, respectively, for 200 min (Fig. 1c). These results showed that only the high CPO concentration induced significant damage to plasma membrane integrity, as previously reported (Sigle *et al.*, 2005), whereas for 18 μg mL^{-1} CPO, the plasma membrane damage was

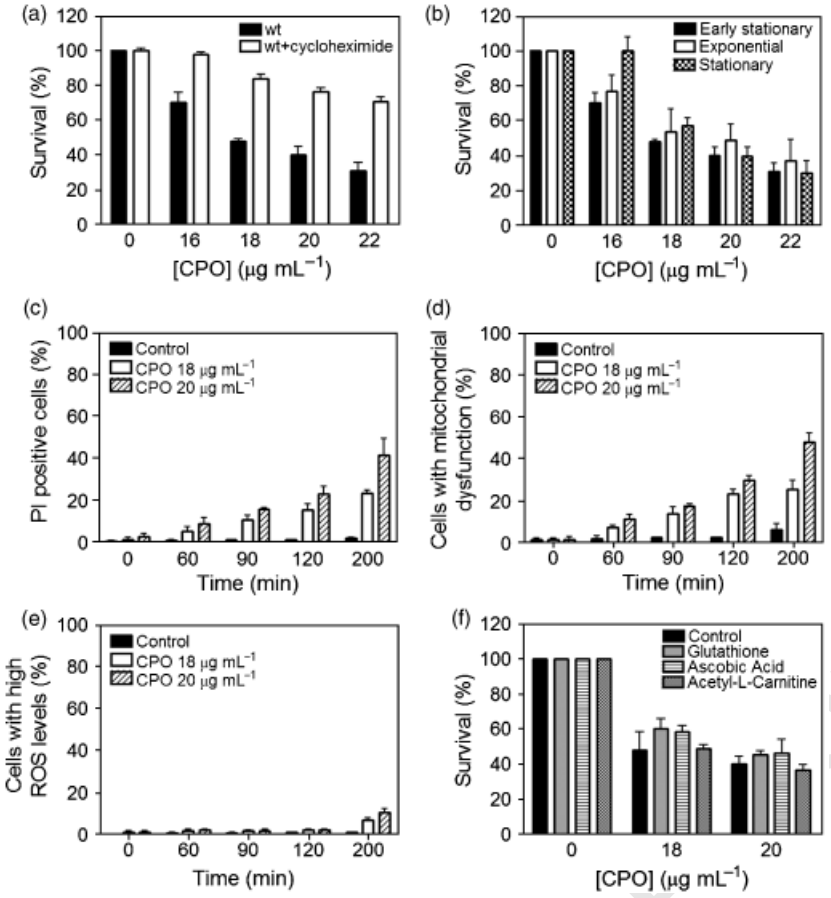

Fig. 1. CPO treatment of wild-type *Saccharomyces cerevisiae* cells results in cell death independent of ROS production with minor alterations in plasma membrane integrity and mitochondrial membrane function/integrity. (a) Effect of cycloheximide on the survival of *Saccharomyces cerevisiae* cells treated for 200 min with different CPO concentrations. (b) Survival rate of exponential-phase, early stationary-phase and stationary-phase cells with different CPO concentrations, after 200 min of treatment. (c) Percentage of cells displaying affected plasma membrane integrity as assessed by flow cytometric quantification of cells after vital staining with PI. (d) Percentage of cells presenting mitochondrial dysfunction as assessed by flow cytometric quantification of cells with increased levels of Rh123. (e) Percentage of cells with increased ROS levels, as assessed by flow cytometry using the fluorescent probe MitoTracker Red CM-H_2XRos. (f) Survival rate of CPO-treated *Saccharomyces cerevisiae* cells evaluated in the absence (control) and presence of different classes of ROS scavengers. Vertical error bars representSD.

considerably lower in comparison to the observed cell death (Fig. 1a and c). Nonetheless, alterations at the plasma membrane functional level were not evaluated, and therefore their occurrence could not be completely discounted.

Mitochondria are preferential targets for the majority of antifungal agents. Azoles are the best example, because in addition to their action at the plasma membrane, they can indirectly affect mitochondria (Kontoyiannis & Murray, 2003). Although CPO acts as a chelator of Fe^{3+} (Wanner *et al.*, 2000; Linden *et al.*, 2003; Niewerth *et al.*, 2003), it seems to be important in the maintenance of mitochondrial membrane potential (Lee *et al.*, 2005b). We therefore assessed yeast mitochondrial function/integrity on the basis of Rh123 staining (Ludovico *et al.*, 2001a). Our results showed that approximately the same percentage of PI-positive cells displayed loss of mitochondrial function/integrity (Fig. 1d). The results obtained with the study of plasma and of mitochondrial membrane integrity after 200 min of 18 μg mL^{-1} CPO treatment suggested that some cells were being killed by an active process, and prompted us to analyze the nuclear morphology and chromatin condensation of yeast cells exposed to CPO. The ultrastructural analyses performed by TEM together with DAPI staining showed that CPO induced chromatin condensation and changes in nuclear morphology, respectively (Fig. 2b). Moreover, CPO induced the appearance of a subpopulation displaying a decrease in forward scatter (directly correlated with cell size) as evaluated by flow cytometry (Fig. 2c). Cell sorting of this subpopulation showed small cells with compromised plasma membrane integrity but that maintained their genome size, as shown by their cell cycle profile (Fig. 2c). Moreover, as revealed by CFU counts, these cells had lost their proliferation capacity (data not shown).

The results described above, namely (1) dependence of cell death on protein synthesis, (2) maintenance of plasma membrane integrity and of mitochondrial function/integrity, (3) chromatin condensation, and (4) nuclear morphologic changes observed for the majority of *S. cerevisiae* cells, when treated with 18 μg mL^{-1} CPO, fit with a scenario of an ACD process triggered by CPO. On the other hand cells treated for 200 min with 20 μg mL^{-1} CPO already displayed a phenotype compatible with necrosis that might also correspond to the final stages of the ACD process, as previously described for high concentrations of acetic acid (Ludovico *et al.*, 2001b) or hydrogen peroxide (Madeo *et al.*, 1999).

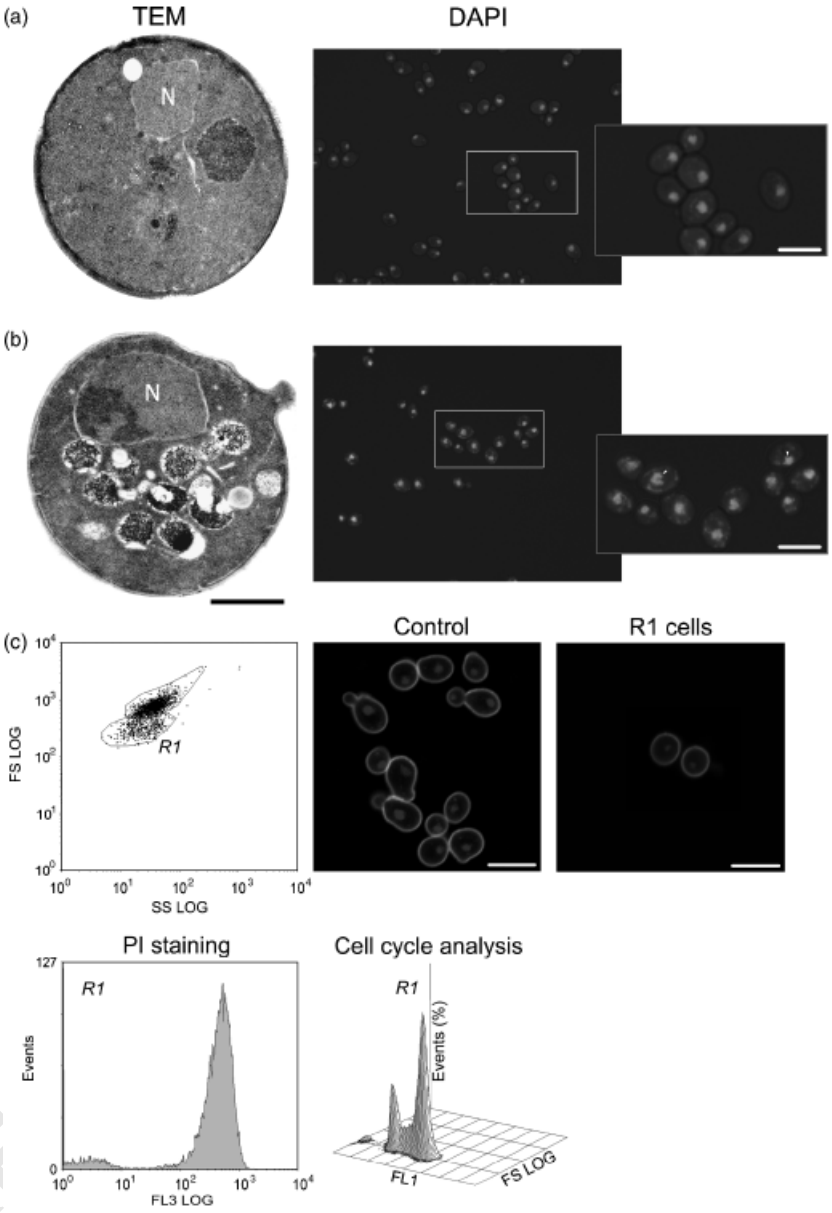

Fig. 2. CPO induces nuclear morphologic alterations, chromatin condensation and the appearance of a subpopulation with a decreased forward scatter and compromised plasma membrane integrity. TEM and epifluorescence micrographs (DAPI staining) of (a) untreated and (b) CPO-treated cells (18 μg mL^{-1}, 200 min). N, nuclei. (C) Confocal micrographs of sorted cells (from control and R1 subpopulation, displaying a decrease in forward scatter), double stained with DAPI and ConA (incubation with 0.2 mg mL^{-1} ConA, 30 min at room temperature), displaying compromised plasma membrane integrity but a normal cell cycle profile [density plot, three-dimensional profile analysis of forward scatter (FS) log, green fluorescence (FL1) and percentage of events]. Bar, 5 μm (1 μm for TEM micrographs).

CPO-induced cell death is independent of ROS

To further characterize the cell death process triggered by CPO, several yeast apoptotic regulators were studied. ROS are known to be crucial mediators of yeast apoptosis, being associated with the vast majority of apoptotic phenotypes described so far (reviewed in Madeo *et al.*, 2004). Surprisingly, a kinetic study using CPO concentrations of 18 and 20 μg mL^{-1}, which induce, respectively, about 50% and 60% loss of viability (Fig. 1a), revealed that only a very low percentage of CPO-treated cells displayed high intracellular ROS concentrations, reaching a value of about 10% for the highest concentration (20 μg mL^{-1}) after 200 min of treatment (Fig. 1e). These results might be explained by CPO's ability to function as an iron chelator (Daudu *et al.*, 2002). Iron is an essential cofactor for mitochondrial electron transport enzymes as well as for the Fenton reaction, which might cooperate to inhibit ROS production. Furthermore, CPO treatment in the presence of different classes of ROS scavengers did not enhance cell survival (Fig. 1f). For longer CPO incubation times (up to 400 min), an increase of the percentage of cells with high ROS levels was detected but was associated with an increase in cell death that was not prevented by the presence of different ROS scavengers (data not shown). Overall, these data strongly support the view that CPO-induced cell death is independent of ROS signaling.

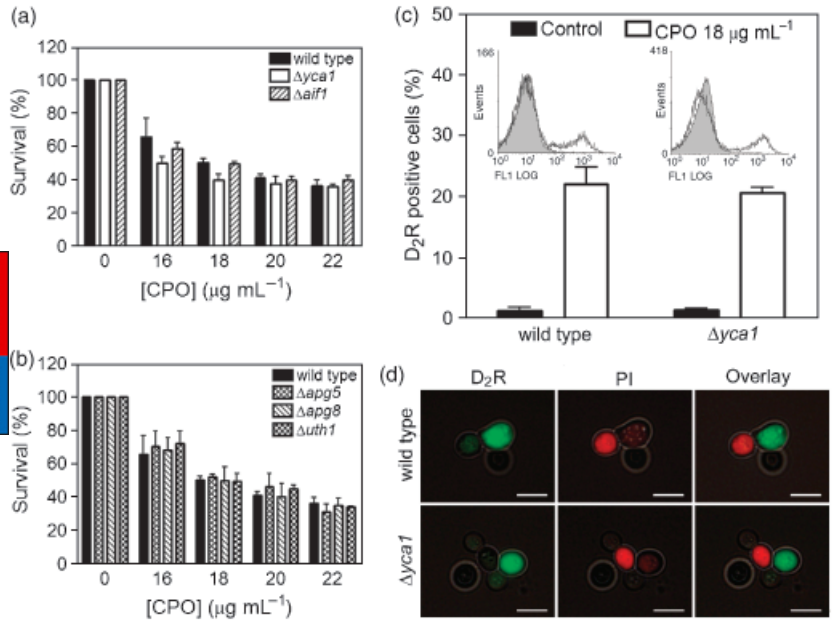

Fig. 3. CPO-induced cell death is independent of *Saccharomyces cerevisiae* apoptotic regulators and of autophagic pathways but is associated with a caspase-like or ASPase activity independent of YCA1. Relative survival, upon CPO treatment, of wild-type and respective knockout cells with different (a) apoptotic and (b) autophagic regulators. (c) Percentages of wild-type and Δ*yca1* cells displaying caspase-like or ASPase activity, assessed by flow cytometric quantification of cells incubated with D_2R. Filled area (gray), untreated cells stained with D_2R. Open area, CPO-treated cells (18 μg mL^{-1}, 200 min). Vertical error bars represent SD. (d) Epifluorescence micrographs of CPO-treated wild-type and Δ*yca1* cells (18 μg mL^{-1}, 200 min), double stained with D_2R and PI. Bar, 5 μm.

CPO-induced cell death is independent of known yeast apoptotic regulators and has a TUNEL-negative phenotype

The involvement of known *S. cerevisiae* apoptotic regulators (reviewed in Ludovico *et al.*, 2005), namely apoptosis-inducing factor (AIF1) and metacaspase (YCA1), was analyzed under CPO-induced cell death conditions. As a first approach, survival after CPO treatment was estimated in each mutant strain in comparison with the wild-type strain. The results (Fig. 3a) showed that there were no differences between the survival percentages obtained for each of the mutant strains, indicating that the respective proteins do not have a significant role in the signaling and/or execution of the CPO-induced cell death process. However, *c.* 20–25% of the wild-type cells exposed to 18 μg mL^{-1} CPO were labeled by the D_2R substrate [$(Asp)_2$-rhodamine 110], which enabled the determination of cells with intracellular caspase-like or other ASPase activities (Fig. 3c). Nonetheless, an identical level of D_2R labeling was observed in *Δyca1* cells treated with 18 μg mL^{-1} CPO (Fig. 3c), indicating that an ASPase activity independent of YCA1 was present. Moreover, Z-VAD-FMK was unable to block the observed ASPase activity in either wild-type or Δ*yca1* cells (data not shown), pointing to the presence of a caspase-like or other protease that was insensitive to Z-VAD-FMK inhibition, as shown by others (Váchová & Palková, 2005).

The number of cells displaying caspase-like or ASPase activity is quite similar to the percentage of PI-positive cells under the same conditions (about 23% for 18 μg mL^{-1} CPO). However, D_2R staining was previously described to be a good alternative for detection of caspase-like or ASPase activity in living yeast cells (Váchová & Palková, 2005). Accordingly, our results show that D_2R and PI stain different cells (Fig. 3d). Altogether, our findings led us to hypothesize that other unknown protease(s) could be involved in the CPO-induced cell death of *S. cerevisiae*, as recently proposed in different instances (Herker *et al.*, 2004; Váchová & Palková, 2005). Another intriguing deviation from a typical apoptotic cell death process was the observation that CPO-treated cells had no TUNEL-positive phenotype (data not shown).

CPO-induced yeast cell death is not autophagic

In order to obtain new insights into the puzzling cell death pathway induced by CPO in *S. cerevisiae* cells, we considered the possibility of this cell death process being autophagic, as CPO induces an increase in vacuolization observed by TEM (Fig. 2b). Both Apg5p and Apg8p are crucial for the formation of the preautophagosomal structure in yeast cells (Suzuki *et al.*, 2001), and Uth1p is required for the autophagic degradation of mitochondria (Camougrand *et al.*, 2004). In this regard, the susceptibilities of the Δ*apg5*, Δ*apg8* and Δ*uth1* mutant strains were assessed after CPO treatment. None of the tested mutant strains was shown to have a different susceptibility to CPO treatment when compared to the wild-type strain (Fig. 3b). In addition, blocking autophagy with 3-methyladenine (Seglen & Gordon, 1982) did not inhibit CPO-induced cell death (data not shown). Altogether, these results indicate that the autophagic pathways analyzed are not involved in CPO-induced cell death.

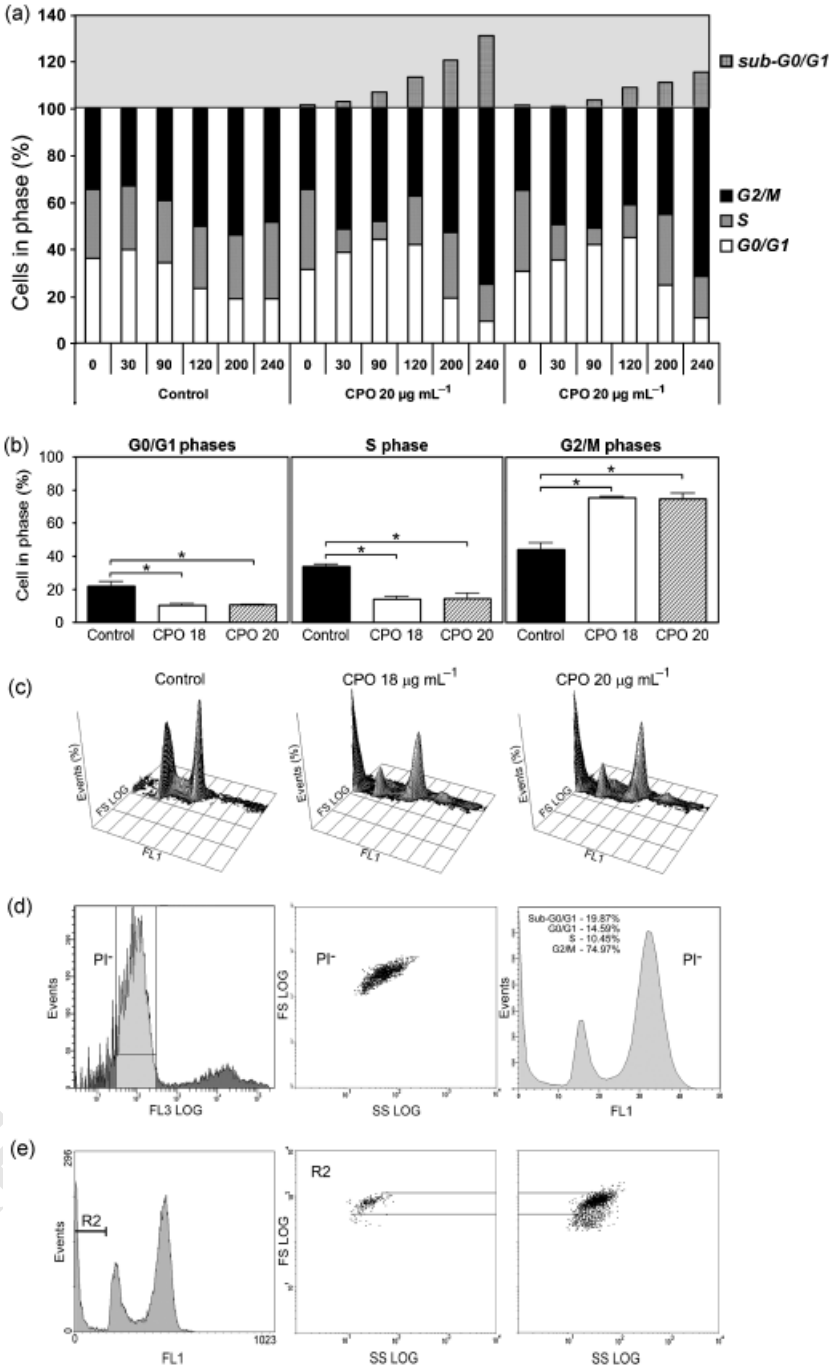

Fig. 4. CPO induces the appearance of a sub-G_0/G_1 population and G_2/M arrest/delay. (a) Kinetic analysis of the percentage of *Saccharomyces cerevisiae* cells in each phase of the cell cycle. (b) Percentage of untreated (control) and CPO-treated (18 and 20 μg mL^{-1}) *Saccharomyces cerevisiae* cells in each phase of the cell cycle after 240 min of treatment; $^*P \leq 0.05$ vs. control, *t*-test, $n = 3$. (c) Density plot of three-dimensional profile analysis of forward scatter (FS log), green fluorescence (FL1) and percentage of events of untreated (control) and CPO-treated (18 and 20 μg mL^{-1}) *Saccharomyces cerevisiae* cells after 200 min of treatment. (d) Left panel: Histogram of logarithmic FL3 (red fluorescence) of PI-stained cells (treated with 18 μg mL^{-1} CPO, 200 min) displaying PI-negative cells (gray color) used for cell sorting. Middle panel: Dot plot of logarithmic forward scatter (FS log) vs. logarithmic side scatter (SS log) of CPO-treated (18 μg mL^{-1}, 200 min) *Saccharomyces cerevisiae* PI-negative cells. Right panel: Cell cycle profile of PI-negative CPO-treated (18 μg mL^{-1}, 200 min) cells. (e) Left panel: Cell cycle profile of CPO-treated (18 μg mL^{-1}, 200 min) cells, displaying a sub-G_0/G_1 subpopulation (R2). Middle panel: Dot plot of logarithmic forward scatter (FS log) vs. logarithmic side scatter (SS log) of *Saccharomyces cerevisiae* cells from the R2 subpopulation. Right panel: Dot plot of logarithmic forward scatter (FS log) vs. logarithmic side scatter (SS log) of CPO-treated (18 μg mL^{-1}, 200 min) cells.

CPO induces the appearance of a sub-G_0/G_1 population and G_2/M arrest/delay

As a consequence of exposure to diverse cytotoxic agents, DNA damage can occur, leading to an arrest in the cell cycle and, ultimately, to cell death. DNA damage checkpoints are critical for the fate of the cell, allowing DNA damage detection and repair or, when injury is too extensive, cell death (Tyson *et al.*, 2002). As the mechanism of DNA repair was shown to be one of the targets of CPO (Leem *et al.*, 2003), the effect of CPO on cell cycle progression was assessed through a flow cytometric determination of DNA content (Fig. 4a). Leem *et al.* (2003) previously reported for another *S. cerevisiae* strain that CPO treatment induces a general growth arrest at different points of cell cycle. Our results showed that CPO treatment induced a statistically significant arrest/delay in the G_2/M phases of the cell cycle (Fig. 4a and b). In addition, CPO treatment induced the

appearance of a subpopulation of cells with a lower DNA content, described as a sub-G_0/G_1 peak (Fig. 4c), which was previously associated with UV-induced yeast apoptosis (Del Carratore *et al.*, 2002). Interestingly, the percentage of cells in sub-G_0/G_1 reaches its highest value for a CPO concentration of 18 $\mu g\,mL^{-1}$. In order to exclude artefacts from the debris associated with necrotic dying cells, which might produce values on the histogram with a sub-G_0/G_1 DNA content, PI-negative cells were sorted after treatment with 18 $\mu g\,mL^{-1}$ CPO (Fig. 4d, left panel). Cell cycle analysis of this population revealed the appearance of *c.* 20% of cells in the sub-G_0/G_1 peak (Fig. 4d, right panel). Moreover, when the sub-G_0/G_1 peak was gated and the physical scatter displayed (Fig. 4e, left panel), it was possible to observe that the cells with lower DNA content had a normal physical scatter and did not correspond with either debris or the observed cells with a lower forward scatter. These results strongly support the observed nuclear alterations and concur with the main conclusion that an unknown ACD process is induced by CPO.

CPO triggers an atypical ACD pathway

Altogether, our results show that CPO induces an atypical ACD process in *S. cerevisiae*. This process is dependent on protein synthesis, and is characterized by DNA damage as reflected by cell cycle analysis and the appearance of a sub-G_0/G_1 population, nuclear morphologic alterations, and chromatin condensation. However, this ACD process does not display a TUNEL-positive phenotype and is independent of the known yeast apoptotic regulators, namely AIF1 and YCA1. The detection of non-necrotic wild-type and Δ*yca1* cells labeled by D_2R suggests that this ACD process is mediated by other unknown proteases, as proposed in other scenarios (Herker *et al.*, 2004; Váchová & Palková, 2005). The specific percentage of cells labeled by D_2R substrate is in agreement with the percentage of sub-G_0/G_1 cells, reinforcing the idea that about 25% of the cells treated with CPO (18 $\mu g\,mL^{-1}$) are dying as a result of an atypical ACD process. Moreover, CPO-induced yeast cell death was not associated with ROS signaling, as initially described in other instances (Cheng *et al.*, 2003; Balzan *et al.*, 2004). Although further studies need to be performed, the data presented here highlight the use of CPO for research on the identification of novel proteases and pathways involved in yeast ACD. Additionally, the elucidation of cell death pathways triggered by antifungal drugs may allow the design of new drugs and the rational use of those available.

Acknowledgements

The authors would like to thank A. Salvador for his expertise in cell cycle profile analysis. This work was supported by grants from FCT (Fundação para a Ciência e a Tecnologia), Portugal (POCI/SAU-ESP/61080/2004 and POCI/BIA-BCM/57364/2004) and from Fundação Calouste Gulbenkian, Serviço de Saúde e Desenvolvimento Humano, Portugal (Proc/60666-MM/734). BA has a fellowship from FCT (SFRH/BD/15317/2005).

References

Abrams BB, Hanel H & Hoehler T (1991) Ciclopirox olamine: a hydroxypyridone antifungal agent. *Clin Dermatol* **9**: 471–477.

Balzan R, Sapienza K, Galea DR, Vassallo N, Frey H & Bannister WH (2004) Aspirin commits yeast cells to apoptosis depending on carbon source. *Microbiology* **150**: 109–115.

Byers B & Goetsch L (1991) Preparation of yeast cells for thin-section electron microscopy. *Methods Enzymol* **194**: 602–608.

Camougrand N, Kissova I, Velours G & Manon S (2004) Uth1p: a yeast mitochondrial protein at the crossroads of stress, degradation and cell death. *FEMS Yeast Res* **5**: 133–140.

Cheng J, Park TS, Chio LC, Fischl AS & Ye XS (2003) Induction of apoptosis by sphingoid long-chain bases in *Aspergillus nidulans*. *Mol Cell Biol* **23**: 163–177.

Daudu PA, Roy A, Rozanov C, Mokashi A & Lahiri S (2002) Extra- and intracellular free iron and the carotid body responses. *Respir Physiol Neurobiol* **130**: 21–31.

de la Fuente JM, Alvarez A, Nombela C & Sanchez M (1992) Flow cytometric analysis of *Saccharomyces cerevisiae* autolytic mutants and protoplasts. *Yeast* **8**: 39–45.

Del Carratore R, Della Croce C, Simili M, Taccini E, Scavuzzo M & Sbrana S (2002) Cell cycle and morphological alterations as indicative of apoptosis promoted by UV irradiation in *S. cerevisiae*. *Mutat Res* **513**: 183–191.

Fortuna M, Sousa MJ, Corte-Real M, Leao C, Salvador A & Sansonetty F (2000) *Cell Cycle Analysis of Yeast using Syber Green I* (Robinson JP, eds), pp. 11.13.11–11.13.19. John Wiley & Sons, Inc, New York.

Groll AH, De Lucca AJ & Walsh TJ (1998) Emerging targets for the development of novel antifungal therapeutics. *Trends Microbiol* **6**: 117–124.

Gupta AK (2001) Ciclopirox: an overview. *Int J Dermatol* **40**: 305–310.

Herker E, Jungwirth H, Lehmann KA, Maldener C, Frohlich KU, Wissing S, Buttner S, Fehr M, Sigrist S & Madeo F (2004) Chronological aging leads to apoptosis in yeast. *J Cell Biol* **164**: 501–507.

Iwata K & Yamaguchi H (1981) [Studies on the mechanism of antifungal action of ciclopiroxolamine/Inhibition of transmembrane transport of amino acid, K+ and phosphate in *Candida albicans* cells (author's transl)]. *Arzneimittelforschung* **31**: 1323–1327.

Kokjohn K, Bradley M, Griffiths B & Ghannoum M (2003) Evaluation of *in vitro* activity of ciclopirox olamine, butenafine HCl and econazole nitrate against dermatophytes, yeasts and bacteria. *Int J Dermatol* **42** (Suppl 1): 11–17.

Kontoyiannis DP & Murray PJ (2003) Fluconazole toxicity is independent of oxidative stress and apoptotic effector mechanisms in *Saccharomyces cerevisiae*. *Mycoses* **46**: 183–186.

Lee RE, Liu TT, Barker KS, Lee RE & Rogers PD (2005a) Genome-wide expression profiling of the response to ciclopirox olamine in *Candida albicans*. *J Antimicrob Chemother* **55**: 655–662.

Lee SJ, Jin Y, Yoon HY, Choi BO, Kim HC, Oh YK, Kim HS & Kim WK (2005b) Ciclopirox protects mitochondria from hydrogen peroxide toxicity. *Br J Pharmacol* **145**: 469–476.

Leem SH, Park JE, Kim IS, Chae JY, Sugino A & Sunwoo Y (2003) The possible mechanism of action of ciclopirox olamine in the yeast *Saccharomyces cerevisiae*. *Mol Cells* **15**: 55–61.

Linden T, Katschinski DM, Eckhardt K, Scheid A, Pagel H & Wenger RH (2003) The antimycotic ciclopirox olamine induces HIF-1alpha stability, VEGF expression, and angiogenesis. *Faseb J* **17**: 761–763.

Ludovico P, Sansonetty F & Corte-Real M (2001a) Assessment of mitochondrial membrane potential in yeast cell populations by flow cytometry. *Microbiology* **147**: 3335–3343.

Ludovico P, Sousa MJ, Silva MT, Leao C & Corte-Real M (2001b) *Saccharomyces cerevisiae* commits to a programmed cell death process in response to acetic acid. *Microbiology* **147**: 2409–2415.

Ludovico P, Rodrigues F, Almeida A, Silva MT, Barrientos A & Corte-Real M (2002) Cytochrome c release and mitochondria involvement in programmed cell death induced by acetic acid in *Saccharomyces cerevisiae*. *Mol Biol Cell* **13**: 2598–2606.

Ludovico P, Madeo F & Silva M (2005) Yeast programmed cell death: an intricate puzzle. *IUBMB Life* **57**: 129–135.

Madeo F, Frohlich E, Ligr M, Grey M, Sigrist SJ, Wolf DH & Frohlich KU (1999) Oxygen stress: a regulator of apoptosis in yeast. *J Cell Biol* **145**: 757–767.

Madeo F, Herker E, Wissing S, Jungwirth H, Eisenberg T & Frohlich KU (2004) Apoptosis in yeast. *Curr Opin Microbiol* **7**: 655–660.

Niewerth M, Kunze D, Seibold M, Schaller M, Korting HC & Hube B (2003) Ciclopirox olamine treatment affects the expression pattern of *Candida albicans* genes encoding virulence factors, iron metabolism proteins, and drug resistance factors. *Antimicrob Agents Chemother* **47**: 1805–1817.

Phillips AJ, Sudbery I & Ramsdale M (2003) Apoptosis induced by environmental stresses and amphotericin B in *Candida albicans*. *Proc Natl Acad Sci USA* **100**: 14327–14332.

Sakurai K, Sakaguchi T, Yamaguchi H & Iwata K (1978a) Studies on uptake of 6-cyclohexyl-1-hydroxy-4-methyl-2(1 H)-pyridone ethanolamine salt (Hoe 296) by *Candida albicans*. *Chemotherapy* **24**: 146–153.

Sakurai K, Sakaguchi T, Yamaguchi H & Iwata K (1978b) Mode of action of 6-cyclohexyl-1-hydroxy-4-methyl-2(1 H)-pyridone ethanolamine salt (Hoe 296). *Chemotherapy* **24**: 68–76.

Seglen PO & Gordon PB (1982) 3-Methyladenine: specific inhibitor of autophagic/lysosomal protein degradation in isolated rat hepatocytes. *Proc Natl Acad Sci USA* **79**: 1889–1892.

Sigle HC, Thewes S, Niewerth M, Korting HC, Schafer-Korting M & Hube B (2005) Oxygen accessibility and iron levels are critical factors for the antifungal action of ciclopirox against *Candida albicans*. *J Antimicrob Chemother* **55**: 663–673.

Silva MT, Appelberg R, Silva MN & Macedo PM (1987) *In vivo* killing and degradation of *Mycobacterium aurum* within mouse peritoneal macrophages. *Infect Immun* **55**: 2006–2016.

Suzuki K, Kirisako T, Kamada Y, Mizushima N, Noda T & Ohsumi Y (2001) The pre-autophagosomal structure organized by concerted functions of APG genes is essential for autophagosome formation. *Embo J* **20**: 5971–5981.

Theis T & Stahl U (2004) Antifungal proteins: targets, mechanisms and prospective applications. *Cell Mol Life Sci* **61**: 437–455.

Tyson JJ, Csikasz-Nagy A & Novak B (2002) The dynamics of cell cycle regulation. *Bioessays* **24**: 1095–1109.

Váchová L & Palková Z (2005) Physiological regulation of yeast cell death in multicellular colonies is triggered by ammonia. *J Cell Biol* **169**: 711–717.

Wanner RM, Spielmann P, Stroka DM, Camenisch G, Camenisch I, Scheid A, Houck DR, Bauer C, Gassmann M & Wenger RH (2000) Epolones induce erythropoietin expression via hypoxia-inducible factor-1 alpha activation. *Blood* **96**: 1558–1565.

Author Query Form

Journal	**FEMSYR**
Article	**188**

Dear Author,

During the copy-editing of your paper, the following queries arose. Please respond to these by marking up your proofs with the necessary changes/additions. Please write your answers clearly on the query sheet if there is insufficient space on the page proofs. If returning the proof by fax do not write too close to the paper's edge. Please remember that illegible mark-ups may delay publication.

Query No.	Description	Author Response
Q1	AU: Please define YEPD.	
Q2	AU: 'The green and red fluorescences were collected through a 488-nm blocking filter, a 550-nm long-pass dichroic-1 with a 525-nm bandpass-1 and a 590-nm long-pass-1 with a 620-nm bandpass-1, respectively.' The exact meaning of this sentence is not clear. You seem to list three items, but the 'respectively' refers back to two items (green and red). Also, you use adjectives without nouns: 'dichroic' and 'long -pass'. Please clarify.	
Q3	AU: Please define D_2R.	
Q4	AU: Fig. 2c. Please note that figures should normally be cited in number order; is there a particular reason why Fig. 2 is cited before Fig. 1?	
Q5	AU: Please define ConA.	
Q6	AQ: The quality of figure 4d and f is not good for print version. Text and image is unsharpen. Please provide good quality figure	